

Ccn2 deletion predisposes to aortic aneurysm formation and death in mice which is partially reduced by mineralocorticoid receptor antagonist treatment

Raúl Rodrigues Díez¹, Antonio Tejera-Muñoz¹, Vanesa Esteban², Lasse Steffensen³, Raquel Rodrigues-Diez⁴, Macarena Orejudo⁵, Sandra Rayego Mateos⁵, Lucas Falke⁶, Pablo Cannata⁵, Alberto Ortiz⁵, Jesús Egido⁷, Ziad Mallat⁸, Ana Briones⁴, Maria Bajo⁹, Roel Goldschmeding¹⁰, and Marta Ruiz-Ortega⁵

¹Instituto de Investigación Sanitaria de la Fundación Jiménez Díaz

²Instituto de Investigación Sanitaria de la Fundación Jiménez Díaz

³University of Southern Denmark. Unit of Cardiovascular and Renal Research

⁴Universidad Autónoma de Madrid

⁵Instituto de Investigación Sanitaria-Fundación Jiménez Díaz (IIS-FJD)

⁶University Medical Center Utrecht

⁷IIS-Fundación Jiménez Díaz

⁸University of Cambridge

⁹Instituto de Investigación- Hospital universitario La Paz

¹⁰Utrecht University

July 4, 2021

Abstract

Background and Purpose: Cellular Communication Network Factor 2 (CCN2) is a matricellular protein normally present in the vascular wall but overexpressed in several cardiovascular diseases. CCN2 has been proposed as a downstream mediator of profibrotic actions of Transforming Growth Factor (TGF)- β and Angiotensin II (Ang II). However, its direct role in cardiovascular diseases is not completely understood. **Experimental Approach:** To investigate the direct role of CCN2 under vascular pathological conditions, a conditionally deficient CCN2 (CCN2-KO) mouse was evaluated infused or not with Ang II. **Key Results:** In the absence of CCN2, Ang II infusion induced a rapid (within 48 hours) aortic aneurysm generation and increased aneurysm rupture with 80 % lethality at the endpoint. CCN2 deletion caused elastin layer disruption and increased metalloproteinase activity, which were aggravated by Ang II administration. Aortic RNA-seq studies and the subsequent Gene Ontology enriched analysis pointed out the aldosterone biosynthesis process as one of the most enriched terms in absence of CCN2. Pharmacological aldosterone pathway intervention in Ang II-infused CCN2-KO mice, by treatment with the mineralocorticoid receptor antagonist spironolactone, reduced aneurysm formation and mortality after Ang II infusion. **Conclusion and Implications:** CCN2 deletion induces a rapid aneurysm formation and rupture after Ang II infusion which is partially prevented by blocking the mineralocorticoid receptor. Our present data highlight, for the first time, the potential role of CCN2 as a vascular homeostatic factor and its relevance in the aldosterone synthesis, opening new avenues to future studies in aortic aneurysm treatment.

INTRODUCTION

The Cellular Communication Network Factor 2 (CCN2), previously known as connective tissue growth factor (CTGF), belongs to the CCN family (Perbal et al., 2018; Chaqour, 2020), composed also by CCN1/Cyr61

(cysteine rich protein), CCN3/Nov (nephroblastoma overexpressed protein) and other three secreted proteins (CCN4-6). These matricellular proteins share a structural tetramodular organization and are important extracellular matrix (ECM) components involved in the regulation of different cellular functions (Perbal, 2004; Leask and Abraham, 2006; Perbal et al., 2018).

CCN2 exerts multiple context-dependent biological functions, including regulation of cell growth, differentiation, development, adhesion, inflammation and ECM remodeling (Perbal, 2004). Regarding the cardiovascular system, CCN2 is highly expressed during development in heart, branchial arches, and in endothelium and vascular smooth muscle cells (VSMCs) of major blood vessels (Ivkovic et al., 2003; Ponticos, 2013) and it is overexpressed in experimental and human cardiovascular diseases, like heart failure, pulmonary hypertension, restenosis and atherosclerosis (Perbal, 2004; Hall-Glenn et al., 2012; Ponticos, 2013; Rodrigues-Diez et al., 2015). CCN2 plays a relevant role in fibrogenesis, is a well-established marker of fibrosis and has been considered the key downstream profibrotic mediator of Transforming Growth Factor (TGF)- β and of other important factors involved in cardiovascular diseases, such as Angiotensin II (Ang II) (Leask and Abraham, 2006; Ruiz-Ortega et al., 2007a). Based on those studies, CCN2 was proposed as a growth factor and cytokine, but a recent review suggested also the potential relevance of CCN2 in maintaining optimal vascular stiffness, encouraging to further decrypt its contribution to mechanical homeostasis in blood vessels (Chaqour, 2020).

Preclinical studies suggest that CCN2 blockade could be a potential therapeutic option for fibrotic diseases, due to the promising results in experimental liver, lung and renal fibrosis (Luo et al., 2008; Ponticos et al., 2009; Phanish et al., 2010; Hao et al., 2014; Huang et al., 2016) as well as in pulmonary vascular remodeling and heart failure (Wang et al., 2011; Szabó et al., 2014). However, other studies demonstrated that CCN2 upregulation can also exert beneficial effects. Thus, specific CCN2 overexpression in cardiomyocytes protects against the deleterious changes in the heart caused by Ang II-induced pressure overload (Panek et al., 2009) or by ischemia-reperfusion injury (Shakil Ahmed et al., 2011). Accordingly, CCN2 overexpression attenuated myocardial hypertrophy, cardiac dysfunction and left ventricular remodeling in experimental pressure overload and stroke (Gravning et al., 2013). More recently, post-ischemic administration of recombinant CCN2 reduced infarct size and improved cardiac function recovery following ischemia-reperfusion injury (Moe et al., 2016). Due CCN2-KO mice complete embryonic development but die shortly after birth because of respiratory failure (Ivkovic et al., 2003), a conditional CCN2-KO mice have been developed. In this mice, CCN2 deletion ameliorates experimental renal fibrosis (Rayego-Mateos et al., 2018), but does not improve cardiac fibrosis and hypertrophy following transverse aortic constriction (Fontes et al., 2015). High circulating CCN2 levels have been proposed as a potential risk biomarker for cardiac dysfunction in patients with chronic heart failure and myocardial fibrosis (Koitabashi et al., 2008). Moreover, CCN2 mRNA expression was increased in human VSMCs from aneurysms and atherosclerotic plaques (Branchetti et al., 2013; Ponticos, 2013). Nevertheless, scarce information is available about the impact of CCN2 expression modulation in these vascular diseases. OK

Our aim was to further characterize the role of CCN2 in the regulation of vascular responses under normal and pathological conditions, using a conditional CCN2 deficient mouse strain (CCN2^{flox/flox}/Rosa26-ERT/Cre; henceforth named CCN2-KO), and the well-known model of vascular damage induced by systemic Ang II administration (Daugherty et al., 2000) which, in turn, is associated with aortic CCN2 upregulation (Rupérez et al., 2003; Rodrigues-Diez et al., 2013).

METHODS

Experimental model studies

CCN2 deletion: Mice used were CCN2^{flox/flox}/Rosa26-ERT/Cre, henceforth CCN2-KO mice, which are time-conditional knockout (CCN2-KO) mice. They were developed as previously described (Fontes et al., 2015) and used in all experimental models. 13-14 weeks old mice were randomly divided in 2 groups: **1**) CCN2-KO group, in which tamoxifen were intraperitoneally (IP) injected (0.1 ml of a 10mg/mL solution; C8267, Sigma-Aldrich) four times in alternate days and **2**) wild-type (WT) group, which were IP injected with corn

oil (0.1 ml) and used as control group. After two-week washout period, CCN2 deletion was confirmed by polymerase chain reaction (PCR) using CCN2-floxed Forward: 5'- AATACCAATGCACTTGCCTGGATGG-3' and CCN2-floxed Reverse: 5'-GAAACAGCAATTACTACAACGGGAGTGG-3' primers. The amplified DNA was resolved by size in agarose gel (1,5%) (**Suppl Figure 1**).

*Description of experimental models: *For more information see **Suppl Figure 2***

Angiotensin II (Ang II) infusion model . Systemic infusion of Ang II was done using ALZET osmotic mini-pumps (Model 2002, ALZET Alza Corp., Palo Alto, CA) at the dose of 1000 ng/kg/min (A9525, Sigma Aldrich), as previously described (Daugherty et al., 2000; Rodrigues-Diez et al., 2015). Four experimental mice groups were studied: WT (corn oil); WT + Ang II (corn oil and Ang II); CCN2-KO (tamoxifen); and CCN2-KO + Ang II (tamoxifen and Ang II). Several sets of models were done to perform different studies, with at least 5 mice per group. The end point of all experimental models was 15 days of Ang II treatment, except one model used for magnetic resonance imaging (MRI) and Multiple reaction monitoring (MRM) mass spectrometry (MS) studies, which end-point was 5 days after starting Ang II infusion (not shown at models' scheme). To allow MRI studies, the mini-pumps stainless-steel flow moderator was replaced by PEEK Tubing (DURECT Corporation) using the ALZET MRI Compatibility Technical Tip.

Spironolactone treatment on Ang II infusion model: To study the role of aldosterone, some CCN2-KO + Ang II mice were treated with Spironolactone (SP) (S3378-1G, Sigma-Aldrich), a mineralocorticoid receptor antagonist (Liu et al., 2013), dissolved in corn oil at the dose of 50mg/kg/day by IP injection every 48 hours, starting one day prior first tamoxifen injection. Four experimental mice groups were studied in this case: WT (corn oil); CCN2-KO (tamoxifen); CCN2-KO + Ang II (tamoxifen and Ang II) and CCN2-KO + Ang II + Spironolactone (SP) (tamoxifen, Ang II and SP).

Systolic blood pressure measurements

The LE5001 noninvasive blood pressure acquisition system (Panlab, Harvard apparatus) and the appropriated cuff and transducer (76-0432 for mice; Panlab Harvard Apparatus) were used as previously described (Orejudo et al., 2020). Measurements were done in a quiet and temperature regulated area ($\pm 22^{\circ}$ C), being animals preheated (37° C, 10 minutes) before measurements and maintained at 35° C, and having 10 to 15 measurements per animal in each session. Systolic blood pressure is expressed as the mean of 5 to 10 measurements each day, and graphed for the day before first tamoxifen injection, the day of Ang II-osmotic minipumps' surgery and 7 to 15 days since Ang II systemic administration.

Magnetic Resonance Imaging

Magnetic Resonance Imaging (MRI) was used to evaluate the time-course evolution of the aneurysm formation in response to Ang II. MRI assessments were repeated every day for five days (0, 24, 48, 72 and 96 hours from the starting of Ang II infusion). The number of averaged experiments (NA) was 2 and the total acquisition time for this experiment was 12 minutes and 17 seconds. In the most caudal position of the image volume a flow saturation slice was used to eliminate the signal of venous flow. Magnetic Resonance Angiography (MRA) data were processed using ImageJ 1.51 (NIH, Bethesda, Maryland, USA). The aorta areas, comprising aortic wall and lumen, and the lumen areas were measured by two independent observers using ParaVision 3.1 software (Bruker, Ettlingen, Germany). Regions of interest were manually drawn and the mean of the two measurements were calculated. The aortic areas were measured on every 1-mm slice from the superior mesenteric artery to 10 mm above it.

Aortic ultrasound imaging measurements in vivo.

The maximal internal diameters of the thoracic (ascending and descending) (TAsA, TDsA) and abdominal aorta (AbA) were monitored in isoflurane-anesthetized mice at day 0 to end point (see supplemental scheme) using the portable LOGIQ-e Ultrasound system with an L10-22 probe (10–22 MHz; GE Healthcare, Chicago). All recordings were made by two technicians in a blinded manner.

Tissue preparation.

At the end of the procedure, mice were euthanized under anesthesia (Isoflurane, Abbott laboratories, Madrid, Spain). Aortic aneurysm presence was evaluated in all mice at the end point before further process of the aortic tissue. Aortas were collected, placed in cold (4°C) Krebs-Henseleit solution (KHS) (115 mmol/L NaCl, 25 mmol/L NaHCO₃, 4.7 mmol/L KCl, 1.2 mmol/L MgSO₄·7H₂O, 2.5 mmol/L CaCl₂, 1.2 mmol/L KH₂PO₄, 11.1 mmol/L glucose, and 0.01 mmol/L Na₂EDTA, pH7.4). Aortas were processed in different conditions depending on the specific experiment. Due to the low amount of tissue and the different experimental approaches, different experimental groups were used for histological studies, protein evaluation techniques (MRM-MS, Western Blot (WB) and zymography) and RNA-seq studies. For histological studies, suprarenal aortic segments were buffered in 4% paraformaldehyde (PFA, pH= 7.4) and embedded in paraffin. For protein or gene expression studies, tissue was immediately frozen in liquid nitrogen and kept at -80°C until analysis. All the evaluations were done in aortic segments of at least 5 mice per group.

Histological, protein and RNA studies in aorta.

Aortic Histochemistry Staining: Paraffin-embedded aortic sections (4 µm thick) were placed in coated slides, deparaffinized, rehydrated through alcohol gradients (100-95-70% alcohol) and washed in distilled water. To visualize the aortic structure, Hematoxylin-Eosin and Van Gieson staining were performed as previous described (Esteban et al., 2011). Images were obtained using a Leica DMD108 microscope (Leica Microsystems).

Transmission electronic microscopy (TEM). Samples were fixed with a 1% glutaraldehyde-4% formaldehyde solution in 0.1M cacodylate buffer. Post-fixation process consisted on one hour and forty minutes of 1% osmium tetroxide solution incubation at room temperature. Afterwards, samples were washed in distilled water, stained with 0.5% uranyl acetate solution along ten minutes, dehydrated in increasing graded alcohol solutions (30%, 50%, 70%, 95% and 100%) and incubated in acetone. Samples were included into epoxy Durcupan ACM resin (Sigma-Aldrich, Darmstadt, Germany) with increasing proportions of Resin/acetone (1:3, 1:1, 3:1 and pure resin). Samples were polymerized in 60°C oven during 48 hours. Ultrathin slides were obtained by using Leica Ultracut S (60nm), which were included into 200 mesh copper grids and counterstained with uranyl acetate and plump citrate. Slides were visualized by transmission electron microscopy JEOL JEM1010 (100 kV).

Multiple reaction monitoring (MRM) mass spectrometry (MS) analysis. Whole mouse aortas were homogenized, denatured, resolubilized and trypsinized in 50 mmol/L ammonium bicarbonate at 37°C overnight. Tryptic peptides were purified on custom made Poros R2/R3 (Thermo Scientific) micro columns, dried, reconstituted and finally resuspended in 2% acetonitrile, 0.1% formic acid. Tryptic peptide concentration was determined and normalized across samples. Heavy isotope-labelled standard peptides (JPT) were then added to each sample in a 1:1 volume ratio. 2.5 µg endogenous peptide was run for each sample on an Easy-nLC II nano liquid chromatography (LC) system using a C18 trapping column for desalting and a C18 analytical column for peptide separation (Thermo Scientific). Peptides were eluted, ionised and analyzed on a TSQ Vantage triple quadrupole mass spectrometer (Thermo Scientific) in a selected reaction monitoring mode. MRM raw files were processed using Pinpoint 1.3 (Thermo Scientific). The peak area ratio between endogenous and heavy isotope labelled spiked peptide (1-3 peptides per protein) was used for data analysis. Peak area ratios for individual proteins were normalized to GAPDH and ACTB.

Western blot studies were done in whole aorta samples as described (Rodriguez-Vita et al., 2005). Protein content was determined by the bicinchoninic acid method (BCA; ThermoFisher), and protein were loaded and separated on 10-12% polyacrylamide-SDS gels under reducing conditions. Afterwards, proteins were blotted onto nitrocellulose membranes (BioRad), incubated with the corresponding primary and secondary antibodies and developed using the ECL substrate (Millipore). Results were analyzed by LAS 4000 (GE Healthcare) and obtained bands quantified by using the QuantityOne software (BioRad). The primary antibodies employed were MMP-8 (1/500; sc-514803; Santa Cruz Biotechnologies) and GAPDH (1/5000; CB1001; Millipore.).

Zymography. Protein samples were loaded and separated onto 10% polyacrylamide-SDS gels without reducing conditions with 1% of gelatin (Sigma Aldrich). Gels were washed with 2,5% Triton-X 100 three times for

30 minutes, followed by a final distilled water washing for 30 minutes. Gels were incubated in a reaction buffer (50 mmol/L Tris-HCl pH 7.5, 200 mmol/L NaCl, 10 mmol/L CaCl₂) overnight at 37°C with agitation, stained with Coomassie Brilliant-Blue (Sigma Aldrich) during 30 minutes and incubated in a bleaching buffer to release the leftover Coomassie. Results were analyzed by BioRad Gel DocTM EZ Imager in fresh and band densitometry was quantified by using the QuantityOne software (BioRad).

In situ Zymography. For localization of gelatinolytic activity, *in situ* zymography was performed as previously described (Lindblad, 2001). Briefly, 8 µm thick aortic sections were deparaffinized and rehydrated through graded alcohols. Each sample was incubated with substrate (DQgelatin, Invitrogen) overnight in a dark humidity chamber at 37°C. Nuclei were stained with DAPI (1/10000, Sigma-Aldrich) and samples mounted by using ProlongTM Gold antifade reagent (Invitrogen). Fluorescence (Ex/Em 495/515 nm) was visualized in a Leica DM-IRB confocal microscope. In order to verify the contribution of MMPs, control slides were preincubated with 20mM EDTA for 1 hour. 20 mmol/L EDTA was added to substrate solution to be used also as a technique control.

RNA extraction and RNA-sequencing studies. Aortic total mRNA as obtained by the TRIzol method (Invitrogen, Life Technologies, Philadelphia, PA) as previously described (Lavoz et al., 2020). Libraries were prepared according to the instructions of the Kit “NEBNext Ultra Directional RNA Library Prep kit for Illumina” (New England Biolabs), following the protocol “Poly(A) mRNA Magnetic Isolation Module”. RNA quality was evaluated according to RIN numbers, quantified using a RNA 6000 nanoLabChipin an Agilent 2100 Bioanalyzer (ranges 6-7). The input yield of total RNA to start the protocol was 900 ng. The fragmentation time used was 8-15 minutes according to RIN values. The rest of the protocol was performed according to manufacturer instructions. Obtained libraries were validated and quantified by DNA7500 LabChip kit (Agilent 2100 Bioanalyzer). An equimolecular pool (8-10 aortas per group) of libraries were titrated by quantitative PCR using the “Kapa-SYBR FAST qPCR kit forLightCycler480” (KapaBioSystems) and a reference standard for quantification. The pool of libraries was denatured prior to be seeded on a flowcell at a density of 2,2 pmol/L, where clusters were formed and sequenced using a “NextSeq 500 High Output Kit”, in a 1x75 single read sequencing run on a NextSeq500 sequencer. Approximately 50 million pass-filter reads (range 42-54) were produced for each pool of samples and used for further bioinformatics analysis. FASTq files were analyzed using the XploreRNA service from Exiqon-QuiaGen. The obtained results were studied using the Functional Annotation Tool of David database (49,50). **RNA-seq data are available at the NCBI SRA archive with BioProject record PRJNA669604, and BioSample records SAMN16442923; SAMN16442924; SAMN16442925 and SAMN16442926.*

Statistics

Data are expressed as mean ± standard error of the mean (SEM). Normality distribution was tested with Shapiro-Wilk test. Two tailed Student’s test was used to compare two groups, one-way ANOVA was used to compare one variable in multiple groups and two-way ANOVA to compare two variables. Both ANOVA were followed by the corresponding post hoc analyses test. To analyze no-normal distribution data a non-parametric Mann-Whitney or Kruskal-Wallis tests were used. Survival data were analyzed using the log-rank test and aneurysm incidence by the Fisher exact test. GraphPad Prism 8.0 (GraphPad Software, San Diego California USA) was used to perform the statistical analysis. Values of p <0.05 were considered statistically significant.

Study approval

All animal studies were performed in accordance with current European (Directive 2010/63/EU) and National (*Real Decreto* 53/2013) legislation for the Use and Care of Laboratory Animals, and according to the ARRIVE Guidelines. The protocol was approved by the *Instituto de Investigación Sanitaria Fundación Jiménez Díaz* (IIS-FJD) Animal Research Ethical Committee and by the *Comunidad de Madrid* Committee (PROEX 065/18). All animal work took place in the Laboratory of Molecular and Cellular Biology in Renal and Vascular Pathology of the IIS-FJD at the Autónoma University of Madrid.

RESULTS

Angiotensin II induces severe aortic aneurysm formation and dissection in CCN2-KO mice

Ang II infusion in CCN2-KO mice dramatically decreased survival evaluated at the 15-day endpoint (**Figure 1A**). Some of these mice died as early as at day 2, and post-mortem examination revealed that aortic rupture was the cause of death. Visual aortic evaluation at the endpoint revealed that Ang II-infused CCN2-KO mice significantly developed thoracic and abdominal aorta aneurysms (Thoracoabdominal aneurysms: TAAAs) of all types (according to the Crawford/Safi classification) with a 92 % incidence, while the presence of smaller abdominal aneurysms were found in 30% and 8% of CCN2-KO and WT + Ang II mice, respectively (**Figure 1B and C**).

Blood pressure changes were also evaluated. As expected, Ang II administration increased systolic blood pressure in WT mice. However, a similar blood pressure elevation was observed in CCN2-KO mice infused with Ang II for 15 days. On the other hand, in CCN2-KO mice a slight and persistent decrease in systolic blood pressure was observed upon CCN2 deletion (**Figure 1D**).

Acquired CCN2 deficiency alters aortic structure and increases susceptibility to Ang II-induced aneurysm formation

The impact of CCN2 deficiency on aortic remodeling and the time-course of aneurysm formation in response to Ang II were evaluated by *in vivo* magnetic resonance imaging (MRI) in a 1 cm section from the superior mesenteric artery. Angiography analysis confirmed the generation of dissecting aneurysms in CCN2-KO mice in response to Ang II administration, which occurred in some mice as early as at 48 hours (**Figure 2A and Suppl Figure 3**). These aneurysm-related structural changes include patchy reductions of the aortic lumen associated with increased total aortic area (**Figure 2B**), which could result from medial dissection. Maximum total aortic area and minimum aortic lumen were significantly modified in Ang II-infused CCN2-KO mice after 24 and 72 hours of treatment, respectively (**Figure 2C and D**). In another set of mice experiments, aneurysm formation was followed until 15 days by ultrasound imaging. The echography measurements confirmed that Ang II infusion significantly increased the thoracic ascending aorta (TAsA) and abdominal aorta (AbA) diameters, showing the presence of TAAAs (**Figure 3A and B**).

Importantly, the evaluation of CCN2 deletion effect in the aorta in physiological conditions (in the absence of the pathological stimuli Ang II) by both MRI and ultrasound imaging revealed a key role of CCN2 in aortic homeostasis. MRI evaluations in CCN2-KO mice showed a significant but slight increase in the maximal total area and in the minimum aortic lumen compared to WT mice (**Figure 2C and 2D**), indicating aortic dilatation in absence of CCN2. Additionally, ultrasound imaging measurements confirmed this increment in the AbA diameter in CCN2-KO mice compared to WT (**Figure 3A and B**).

Acquired CCN2 deficiency induces aortic elastic layer disruption that are more severe in Ang II-infused mice

To further determine the impact of CCN2 deficiency on aortic structure, aortic sections were first evaluated by histological techniques. In CCN2-KO mice infused with Ang II, aneurysmal lesions were characterized by elastic lamina rupture and aortic wall dissection with extravasation of red blood cells outside the muscle layer forming a neo-lumen. Aneurysms also presented inflammatory cell infiltration in the border of the dissected aortic wall, along with reduced cellularity of the muscular layer (**Figure 4A**). Interestingly, Van Gieson staining revealed some areas with disruption of elastic layers in the aortic wall of CCN2-KO mice, both in untreated and Ang II-treated mice, as well as elastic layer thinning or absence in aortic aneurysm sections (**Figure 4B, arrows**). Ultrastructural electron microscopy studies of the aorta showed abnormalities in the elastic laminae. Thus, WT aortas displayed continuous elastic laminae with a consistent width, while CCN2-KO mice showed variable width and a disrupted architecture, including abnormal collagen distribution (**Figure 4C**).

CCN2 deletion promotes changes in the aortic protein expression pattern

To evaluate changes in aortic protein expression caused by acquired CCN2 deficiency, a panel of 17 proteins related to ECM and/or VSMCs status, including CCN2, was studied by multiple reaction monitoring mass spectrometry (MRM-MS) analysis. CCN2 protein was detected in control aorta, supporting its important

role in vascular structure and functions, as a key ECM component. As observed at the gene expression level (**Suppl Figure 3**), aortic CCN2 protein level was significantly reduced in CCN2-KO mice (**Suppl Table 1**), demonstrating the efficacy of gene targeting. Alpha smooth muscle actin (ACTA2) expression was significantly decreased (around 20% reduction) and myosin heavy chain 9 was significantly increased in CCN2-KO mice, suggesting a CCN2-related regulation of both proteins (**Suppl Table 1**). Interestingly, CCN2 was the most Ang II-upregulated protein in WT mice in our panel (2.36-fold increase), suggesting an important role of CCN2 in Ang II-mediated vascular responses and, therefore, in the aortic protective adaptive response induced after Ang II infusion.

Acquired CCN2 deficiency increases aortic metalloproteinase activity

Matrix metalloproteinases (MMPs) play a key role in aneurysm formation and rupture in several experimental models. To clarify whether CCN2 deletion regulates MMPs levels and/or activity in the aortic wall, a gelatin zymography was performed using protein lysates from the whole aorta. In CCN2-KO mice, MMP-2 and MMP-9 activity was increased compared to WT mice (**Figure 5A**). Ang II infusion further increased this activity both in WT and CCN2 deleted mice. MMP-8 levels were also evaluated by western blot. CCN2 deletion increased relative MMP-8 concentration of both latent and active protein, and this was also observed in response to Ang II administration in WT and CCN2-KO mice (**Figure 5B**). Additionally, the location of increased MMP activity was assessed in thoracic descending aorta sections by *in situ* zymography. In aortas of WT mice, the autofluorescence of elastic layers can be distinguished, and no MMP activity was detected. Ang II administration resulted in local positive MMP-fluorescence (assessed by gelatin-degradation). However, in CCN2-KO mice there was lower elastin-fluorescence but increased MMP-fluorescence between the elastic layers, which was further increased by Ang II (**Figure 5C**).

Acquired CCN2 deficiency induces changes in the aortic gene expression pattern

RNA-sequencing was used to assess aortic transcriptomics changes and to provide insight into the molecular mechanisms involved in CCN2 actions in the vasculature and in aneurysm formation. As expected, a heat map two-way hierarchical clustering of genes and samples showed that CCN2-KO + Ang II mice clearly differed from the other sets of mice (**Figure 6A**), but it also exhibited a different aortic gene expression pattern in the CCN2-KO mice compared to WT group (**Figure 6B**). Although samples were analyzed as pools limiting the statistical power to detect differentially expressed genes (Rajkumar et al., 2015), we used them as hypothesis-generating experiments. To search for potential mechanisms involved in the vascular effects of CCN2 deletion, a GO enrichment analysis was done using the most deregulated genes obtained from the RNA-Seq studies in the WT *vs* . CCN2-KO comparative analysis (67 genes, Q-value < 0.5; fold-change >0.6) (**Table 1**). In this analysis, BP category results identified C21-steroid hormone biosynthetic process, cholesterol metabolic process, steroid biosynthetic and metabolic processes, or aldosterone biosynthetic process as some of the most deregulated terms in absence of CCN2. Regarding the CC level, extracellular region, extracellular space, secretory granule or mitochondrial crista were the standout terms, while Toll-like receptor 4 binding, scaffold protein binding, iron ion binding or oxidoreductase activity terms spotlight in the MF category (**Table 2**).

Mineralocorticoid receptor blockade reduced aneurysm formation induced by Ang II administration in CCN2-KO

As aldosterone biosynthetic process was one of the most BP enriched terms in the deregulated genes from CCN2-KO mice (**Table 2**) we investigated whether aldosterone pathway activation in CCN2 deficient mice could contribute to aneurysm formation and rupture in presence of Ang II. To this purpose, a new experiment included an additional group of CCN2-KO mice treated with the mineralocorticoid receptor antagonist spironolactone in combination with Ang II infusion. As previously described with other mineralocorticoid receptor antagonist, eplerenone, (Kurobe et al., 2013) spironolactone administration did not prevent blood pressure increase induced by Ang II (**Figure 7A**). However, the reduction of aortic aneurysm formation and the improved survival curve in presence of spironolactone suggested a role of aldosterone in this process (**Figure 7B and C**). In line with this finding, spironolactone decreased both MMP-2 and MMP-9 activity

in Ang II-infused CCN2-KO mice (**Figure 7D**).

DISCUSSION AND CONCLUSIONS

Our experimental study shows, for the first time, that acquired CCN2 deficiency potentiates Ang II-induced deleterious effects in the aorta, increasing the risk of life-threatening TAAAs aneurysm formation and dissection. In addition, spironolactone preventive treatment increases the survival rate and decreases aortic aneurysm formation in CCN2-KO mice after Ang II administration, suggesting a main role of the mineralocorticoid receptor signaling in this pathological process. The observed beneficial effects of spironolactone in this new aneurysm-formation experimental model suggest the mineralocorticoid receptor antagonist treatment as a potential therapeutic option in aneurysms-related human pathologies.

CCN2 plays a key role in the regulation of ECM proteins, as observed in embryonic vascular development, regulating elastin and different types of collagen, and stabilizing mature vessels (Chaqour, 2013). Many preclinical studies have demonstrated that CCN2 is involved in fibrotic disorders (Luo et al., 2008; Ponticos et al., 2009; Phanish et al., 2010; Hao et al., 2014; Huang et al., 2016). However, CCN2 modulation can exert opposite effects depending on the pathological conditions, as described in various cardiovascular pathologies (Gravning et al., 2013; Moe et al., 2016). In a previous *in vitro* study, we found that Ang II infusion produced collagen accumulation and CCN2 overexpression in rat aorta, and CCN2 blockade diminished Ang II-induced ECM overproduction in culture vascular smooth muscle cells (Rupérez et al., 2003). At human level, CCN2 upregulation has also been described in aortic aneurysms (Branchetti et al., 2013), and it was associated with collagen deposition in human atherosclerotic lesions and in thoracic aortic dissection (Ponticos, 2013; Meng et al., 2014). Our present findings showing exacerbated aortic aneurysm formation and fatal dissection caused by Ang II in CCN2 deficient mice point out a potential role of CCN2 in the regulation of an adaptive and protective response that maintains aortic wall integrity. The histological evaluations of CCN2-KO mice revealed aortic wall alterations, including elastic layer disruption, which were more severe after Ang II infusion. Elastic fibers are major aortic ECM components, and their degradation or loss alter the mechanical behavior of the aortic wall (Yanagisawa and Wagenseil, 2020). Enzymes involved in ECM degradation, such as MMPs and collagenases, have special relevance in aneurysm formation and rupture (Matthew Longo et al., 2002; Ju et al., 2014; Thirunavukkarasu et al., 2016). Here, we described that acquired CCN2 deficiency increased MMP2 and MMP9 activity, and upregulated MMP8 synthesis. The elevated MMPs activity was located between the elastic layers, coincidentally with elastin loss. Previous studies demonstrated that Ang II increased aortic MMPs activity and elastic layer degradation (Forrester et al., 2018), as we have also found in CCN2-deleted mice. These findings support that MMPs regulation is also an important mechanism in CCN2-mediated aortic wall destabilization and aneurysm formation.

Several observational studies reported dysregulated CCN2 expression in both non-syndromic (Branchetti et al., 2013) and syndromic human thoracic aortic aneurysms, as observed in several heritable connective tissue disorders such as Marfan, Loeys-Dietz, Ehlers-Danlos, aneurysms-osteoarthritis, and the arterial tortuosity syndrome (Zoppi et al., 2018). These pathologies are characterized by altered connective tissue, resulting in perturbed assembly of ECM, maintenance and homeostasis in various organ systems, including blood vessels, heart, bones, eyes, skin or lungs (Zoppi et al., 2018). In some of these syndromes, aneurysms have been linked to TGF β pathway deregulation. Marfan syndrome is caused by mutations in the gene that encodes fibrillin-1, which participates in the maintenance of the large latent complex of TGF β 1 in its inactive state. The Loeys-Dietz Syndrome is associated with heterozygous mutations in the genes encoding TGF β receptors (TGFBR) 1 and 2, and other components of the pathway (TGFB2, TGFB3, SMAD3, and SMAD4) (Loeys et al., 2005). Mutations in those genes are expected to disrupt TGF- β signaling. Paradoxically, increased TGF β signaling was suggested to cause aortic aneurysm development in those syndromes; however, approaches disrupting TGF β in experimental aneurysm models were not protective (Chen et al., 2016; Lareyre et al., 2017; Mallat et al., 2017). In fact, TGF- β blockade, as observed here for CCN2 deletion, exacerbates aneurysm formation and dissection in several experimental models (Wang et al., 2010; Li et al., 2014; Mallat et al., 2017), although full mechanisms have not been completely unraveled. Moreover, although some authors suggested that angiotensin II receptor 1 blockade should be considered in patients with thoracic aortic aneurysms based on

its ability to inhibit TGF β production (Habashi et al., 2006), clinical results are controversial, as losartan did not provide any benefit in Marfan patients but irbesartan was associated with a reduced rate of aortic dilatation in children and young adults with this syndrome. (Lacro et al., 2014; Milleron et al., 2015; Mullen et al., 2019). Interestingly, another study revealed that human abdominal aortic aneurysm was associated with down-regulation of transcripts encoded by a 16-Mbp segment between cytogenetic bands q22.1 and q23.2 of chromosome 6, where only CCN2 was found differentially expressed (Biros et al., 2014). Therefore, authors suggested that CCN2 could be directly related to aneurysm generation in these patients. The present findings show that CCN2 deletion shares similarities to TGF β pathway disruption in aortic aneurysm development, providing a novel framework to explore the pathogenesis of aneurysms and aortic rupture. Thus, our results suggest that the safety of CCN2 blockade should be studied in depth prior to considering it as a therapeutic option in patients predisposed to or presenting aortic aneurysm.

Hypertension is a well-known predisposing risk factor for human thoracic aortic disease (Lemaire and Russell, 2011), although mechanisms involved are not well elucidated. Hypertension resulting from activation of the renin-angiotensin system has been associated with both abdominal and thoracic aortic aneurysms in experimental mice models under certain circumstances, in particular in response to Ang II administration in Apolipoprotein E deficient mice (Trachet et al., 2015). Here, we show that the resistance of young C57Bl/6 mice to Ang II-induced aortic aneurysm is lost in a context of CCN2 deficiency. Importantly, CCN2 deletion did not increase Ang II-induced blood pressure elevation as compared to WT mice, suggesting that the deleterious effects of CCN2 absence are independent on blood pressure regulation. On the contrary, systolic blood pressure decreased in CCN2-KO mice compared to WT mice. These results agree with observations in genetically modified mice of another ECM components such as the extracellular metalloproteinase ADAMTS1. Thus, studies of partial deletion or silencing of this gene, showed that ADAMTS1 reduction was associated to blood pressure decrease and aneurysm formation in response to Ang-II infusion (Oller et al., 2017), as we have observed here in CCN2 deleted mice.

The role of some other CCN family proteins in the pathophysiology of aneurysm generation have been recently described. CCN4 deletion suppressed aneurysm severity in ApoE knockout mice infused with Ang II (Williams et al., 2021). Though CCN3, in the same way as we observe here, seemed to be protective in two different experimental models of aneurysm, induced by elastase and Ang II administration. All these data highlight the functional diversity of these factors. Our results suggest that CCN2 is an important matricellular ECM protein necessary for maintaining the adult vascular wall architecture in health and disease, supporting its key role as a regulator of vascular ECM matrix homeostasis.

One of the most enriched biological process terms in the absence of CCN2 was the aldosterone biosynthetic process, suggesting that aldosterone could participate in the observed aneurysms pathogenesis. Several clinical cases revealed aortic dissection in primary aldosteronism patients (Ahmed et al., 2007). Some studies found an association between mineralocorticoid receptor blockers and slowed aortic aneurysm progression (Thompson et al., 2010; Kurobe et al., 2013). In mice fed a high salt diet, treatment with a mineralocorticoid receptor agonist caused aortic aneurysm formation and rupture (Liu et al., 2013). Here, we demonstrate that mineralocorticoid receptor inhibition by spironolactone reduced aneurysm generation and death induced by Ang II infusion in CCN2-KO mice, without preventing blood pressure elevation. Accordingly, previous studies have described that another mineralocorticoid receptor antagonist, eplerenone, significantly reduced aneurysm development induced by combination of Ang II and β -aminopropionitrile in mice, without affecting blood pressure (Kurobe et al., 2013). Regarding the CCN2-TGF- β connection, there is an interesting relation between aldosterone, the TGF- β pathway and CCN2. Aldosterone increased TGF- β synthesis (Juknevičius et al., 2004; Ruiz-Ortega et al., 2007b) and induced CCN2 in mice cardiomyocytes *in vivo* and in experimental diabetic nephropathy (Han et al., 2006; Messaoudi et al., 2013). By contrast, TGF- β is a potent suppressor of multiple enzymatic steps of steroidogenesis upstream of aldosterone synthesis, with targets including *Cyp11a1*, *Cyp11b1*, *Cyp11b2*, *Cyp21a1*, *NR5A1*, *FDX1*, *FDXR*, *StAR* or *Hsd3b1* (Matsuki et al., 2015). Our findings showed that several of these genes were upregulated in the aorta of CCN2-KO mice, suggesting a similar role of CCN2 in regulating the aldosterone pathway as previously described for TGF- β . Furthermore, our data postulate the involvement of the aldosterone pathway in aortic aneurysm generation and severity,

and support future studies to investigate the potential use of mineralocorticoid receptor antagonists as therapeutic targets in the aneurysm context. OK

In conclusion, we clearly demonstrate, for the first time to our knowledge, that the absence of CCN2 expression predisposes mice to a pathological response to Ang II that favors aneurysm generation and rupture, which is partially mediated by a deregulation of the aldosterone synthesis pathway. Furthermore, considering the well-established connection between TGF- β signaling and CCN2, our current study further supports the importance of the TGF- β pathway in vascular integrity protection against the development and progression of aortic aneurysm and suggests a potential role of the aldosterone pathway in this process. These results open new approaches to study cardiovascular diseases related to connective tissue disorders, especially those associated with vascular abnormalities and aneurysm formation, and sustain the use of mineralocorticoid receptor antagonists as a potential therapeutic approach in their pathogenesis.

SUPPLEMENTAL MATERIALS

Supplemental Figures 1-4

Supplemental Table 1

REFERENCES

- Ahmed, S.H., Husain, N.M., Khawaja, S.N., Massey, C. V., and Pettyjohn, F.S. (2007). Is primary hyperaldosteronism a risk factor for aortic dissection? *Cardiology*.
- Biros, E., Moran, C.S., Walker, P.J., Cardinal, J., and Golledge, J. (2014). A deletion in chromosome 6q is associated with human abdominal aortic aneurysm. *Clin. Sci*.
- Branchetti, E., Poggio, P., Sainger, R., Shang, E., Grau, J.B., Jackson, B.M., et al. (2013). Oxidative stress modulates vascular smooth muscle cell phenotype via CTGF in thoracic aortic aneurysm. *Cardiovasc. Res*.
- Chaqour, B. (2013). Molecular control of vascular development by the matricellular proteins CCN1 (Cyr61) and CCN2 (CTGF). *Trends Dev. Biol*.
- Chaqour, B. (2020). Caught between a “Rho” and a hard place: are CCN1/CYR61 and CCN2/CTGF the arbiters of microvascular stiffness? *J. Cell Commun. Signal*.
- Chen, X., Rateri, D.L., Howatt, D.A., Balakrishnan, A., Moorleghen, J.J., Cassis, L.A., et al. (2016). TGF- β neutralization enhances angii-induced aortic rupture and aneurysm in both thoracic and abdominal regions. *PLoS One*.
- Daugherty, A., Manning, M.W., and Cassis, L.A. (2000). Angiotensin II promotes atherosclerotic lesions and aneurysms in apolipoprotein E-deficient mice. *J. Clin. Invest*.
- Esteban, V., Méndez-Barbero, N., Jiménez-Borreguero, L.J., Roqué, M., Novensá, L., García-Redondo, A.B., et al. (2011). Regulator of calcineurin 1 mediates pathological vascular wall remodeling. *J. Exp. Med*.
- Fontes, M.S.C., Kessler, E.L., Stuijvenberg, L. van, Brans, M.A., Falke, L.L., Kok, B., et al. (2015). CTGF knockout does not affect cardiac hypertrophy and fibrosis formation upon chronic pressure overload. *J. Mol. Cell. Cardiol*.
- Forrester, S.J., Booz, G.W., Sigmund, C.D., Coffman, T.M., Kawai, T., Rizzo, V., et al. (2018). Angiotensin II signal transduction: An update on mechanisms of physiology and pathophysiology. *Physiol. Rev*.
- Gravning, J., Ahmed, M.S., Lueder, T.G. Von, Edvardsen, T., and Attramadal, H. (2013). CCN2/CTGF attenuates myocardial hypertrophy and cardiac dysfunction upon chronic pressure-overload. *Int. J. Cardiol*.
- Habashi, J.P., Judge, D.P., Holm, T.M., Cohn, R.D., Loeys, B.L., Cooper, T.K., et al. (2006). Losartan, an AT1 antagonist, prevents aortic aneurysm in a mouse model of Marfan syndrome. *Science* (80-).

- Hall-Glenn, F., Young, R.A. de, Huang, B.L., Handel, B. van, Hofmann, J.J., Chen, T.T., et al. (2012). CCN2/Connective tissue growth factor is essential for pericyte adhesion and endothelial basement membrane formation during angiogenesis. *PLoS One*.
- Han, K.H., Kang, Y.S., Han, S.Y., Jee, Y.H., Lee, M.H., Han, J.Y., et al. (2006). Spironolactone ameliorates renal injury and connective tissue growth factor expression in type II diabetic rats. *Kidney Int*.
- Hao, C., Xie, Y., Peng, M., Ma, L., Zhou, Y., Zhang, Y., et al. (2014). Inhibition of connective tissue growth factor suppresses hepatic stellate cell activation in vitro and prevents liver fibrosis in vivo. *Clin. Exp. Med*.
- Hoshijima, M., Hattori, T., Aoyama, E., Nishida, T., Yamashiro, T., and Takigawa, M. (2012). Roles of heterotypic CCN2/CTGF-CCN3/NOV and homotypic CCN2-CCN2 interactions in expression of the differentiated phenotype of chondrocytes. *FEBS J*.
- Huang, M., Yang, H., Zhu, L., Li, H., Zhou, J., and Zhou, Z. (2016). Inhibition of connective tissue growth factor attenuates paraquat-induced lung fibrosis in a human MRC-5 cell line. *Environ. Toxicol.*
- Ivkovic, S., Yoon, B.S., Popoff, S.N., Safadi, F.F., Libuda, D.E., Stephenson, R.C., et al. (2003). Connective tissue growth factor coordinates chondrogenesis and angiogenesis during skeletal development. *Development*.
- Ju, X., Ijaz, T., Sun, H., Lejeune, W., Vargas, G., Shilagard, T., et al. (2014). IL-6 regulates extracellular matrix remodeling associated with aortic dilation in a fibrillin-1 hypomorphic mgR/mgR mouse model of severe Marfan syndrome. *J. Am. Heart Assoc*.
- Juknevičius, I., Segal, Y., Kren, S., Lee, R., and Hostetter, T.H. (2004). Effect of aldosterone on renal transforming growth factor- β . *Am. J. Physiol. - Ren. Physiol*.
- Koitaibashi, N., Arai, M., Niwano, K., Watanabe, A., Endoh, M., Suguta, M., et al. (2008). Plasma connective tissue growth factor is a novel potential biomarker of cardiac dysfunction in patients with chronic heart failure. *Eur. J. Heart Fail*.
- Kurobe, H., Hirata, Y., Matsuoka, Y., Sugawara, N., Higashida, M., Nakayama, T., et al. (2013). Protective effects of selective mineralocorticoid receptor antagonist against aortic aneurysm progression in a novel murine model. *J. Surg. Res*.
- Lacro, R. V., Dietz, H.C., Sleeper, L.A., Yetman, A.T., Bradley, T.J., Colan, S.D., et al. (2014). Atenolol versus losartan in children and young adults with Marfan's syndrome. *N. Engl. J. Med*.
- Lareyre, F., Clment, M., Raffort, J., Pohlod, S., Patel, M., Esposito, B., et al. (2017). TGF β (transforming growth factor- β) blockade induces a human-like disease in a nondissecting mouse model of abdominal aortic aneurysm. *Arterioscler. Thromb. Vasc. Biol*.
- Lavoz, C., Rodrigues-Diez, R.R., Plaza, A., Carpio, D., Egido, J., Ruiz-Ortega, M., et al. (2020). VEGFR2 Blockade Improves Renal Damage in an Experimental Model of Type 2 Diabetic Nephropathy. *J. Clin. Med*.
- Leask, A., and Abraham, D.J. (2006). All in the CCN family: Essential matricellular signaling modulators emerge from the bunker. *J. Cell Sci*.
- Lemaire, S.A., and Russell, L. (2011). Epidemiology of thoracic aortic dissection. *Nat. Rev. Cardiol*.
- Li, W., Li, Q., Jiao, Y., Qin, L., Ali, R., Zhou, J., et al. (2014). Tgfr2 disruption in postnatal smooth muscle impairs aortic wall homeostasis. *J. Clin. Invest*.
- Lindblad, W.J. (2001). *Methods in Molecular Biology, Volume 151, Matrix Metalloproteinase Protocols*. Edited by Ian M. Clark. *Anal. Biochem*.
- Liu, S., Xie, Z., Daugherty, A., Cassis, L.A., Pearson, K.J., Gong, M.C., et al. (2013). Mineralocorticoid receptor agonists induce mouse aortic aneurysm formation and rupture in the presence of high salt. *Arterioscler. Thromb. Vasc. Biol*.

- Loeys, B.L., Chen, J., Neptune, E.R., Judge, D.P., Podowski, M., Holm, T., et al. (2005). A syndrome of altered cardiovascular, craniofacial, neurocognitive and skeletal development caused by mutations in TGFBR1 or TGFBR2. *Nat. Genet.*
- Luo, G.H., Lu, Y.P., Song, J., Yang, L., Shi, Y.J., and Li, Y.P. (2008). Inhibition of Connective Tissue Growth Factor by Small Interfering RNA Prevents Renal Fibrosis in Rats Undergoing Chronic Allograft Nephropathy. *Transplant. Proc.*
- Mallat, Z., Ait-Oufella, H., and Tedgui, A. (2017). The Pathogenic Transforming Growth Factor- β Overdrive Hypothesis in Aortic Aneurysms and Dissections: A Mirage? *Circ. Res.*
- Matsuki, K., Hathaway, C.K., Chang, A.S., Smithies, O., and Kakoki, M. (2015). Transforming growth factor beta1 and aldosterone. *Curr. Opin. Nephrol. Hypertens.*
- Matthew Longo, G., Xiong, W., Greiner, T.C., Zhao, Y., Fiotti, N., and Timothy Baxter, B. (2002). Matrix metalloproteinases 2 and 9 work in concert to produce aortic aneurysms. *J. Clin. Invest.*
- Meng, Y., Tian, C., Liu, L., Wang, L., and Chang, Q. (2014). Elevated expression of connective tissue growth factor, osteopontin and increased collagen content in human ascending thoracic aortic aneurysms. *Vascular.*
- Messaoudi, S., Gravez, B., Tarjus, A., Pelloux, V., Ouvrard-Pascaud, A., Delcayre, C., et al. (2013). Aldosterone-specific activation of cardiomyocyte mineralocorticoid receptor in vivo. *Hypertension.*
- Milleron, O., Arnoult, F., Ropers, J., Aegerter, P., Detaint, D., Delorme, G., et al. (2015). Marfan Sartan: A randomized, double-blind, placebo-controlled trial. *Eur. Heart J.*
- Moe, I.T., Ahmed, M.S., Stang, E., Hagelin, E.M.V., and Attramadal, H. (2016). CTGF/CCN2 postconditioning increases tolerance of murine hearts towards ischemia-reperfusion injury Iole jørgen kaasbøll. *PLoS One.*
- Mullen, M., Jin, X.Y., Child, A., Stuart, A.G., Dodd, M., Aragon-Martin, J.A., et al. (2019). Irbesartan in Marfan syndrome (AIMS): a double-blind, placebo-controlled randomised trial. *Lancet.*
- Oller, J., Méndez-Barbero, N., Ruiz, E.J., Villahoz, S., Renard, M., Canelas, L.I., et al. (2017). Nitric oxide mediates aortic disease in mice deficient in the metalloprotease Adamts1 and in a mouse model of Marfan syndrome. *Nat. Med.*
- Orejudo, M., García-Redondo, A.B., Rodrigues-Diez, R.R., Rodrigues-Diez, R., Santos-Sanchez, L., Tejera-Muñoz, A., et al. (2020). Interleukin-17A induces vascular remodeling of small arteries and blood pressure elevation. *Clin. Sci.* 134 :.
- Panek, A.N., Posch, M.G., Alenina, N., Ghadge, S.K., Erdmann, B., Popova, E., et al. (2009). Connective tissue growth factor overexpression in cardiomyocytes promotes cardiac hypertrophy and protection against pressure overload. *PLoS One.*
- Perbal, B. (2004). CCN proteins: Multifunctional signalling regulators. *Lancet.*
- Perbal, B., Tweedie, S., and Bruford, E. (2018). The official unified nomenclature adopted by the HGNC calls for the use of the acronyms, CCN1–6, and discontinuation in the use of CYR61, CTGF, NOV and WISP 1–3 respectively. *J. Cell Commun. Signal.*
- Phanish, M.K., Winn, S.K., and Dockrell, M.E.C. (2010). Connective tissue growth factor-(CTGF, CCN2) - A marker, mediator and therapeutic target for renal fibrosis. *Nephron - Exp. Nephrol.*
- Ponticos, M. (2013). Connective tissue growth factor (CCN2) in blood vessels. *Vascul. Pharmacol.*
- Ponticos, M., Holmes, A.M., Shi-wen, X., Leoni, P., Khan, K., Rajkumar, V.S., et al. (2009). Pivotal role of connective tissue growth factor in lung fibrosis: MAPK-dependent transcriptional activation of type I collagen. *Arthritis Rheum.*

- Rajkumar, A.P., Qvist, P., Lazarus, R., Lescai, F., Ju, J., Nyegaard, M., et al. (2015). Experimental validation of methods for differential gene expression analysis and sample pooling in RNA-seq. *BMC Genomics*.
- Rayego-Mateos, S., Morgado-Pascual, J.L., Rodrigues-Diez, R.R., Rodrigues-Diez, R., Falke, L.L., Mezzano, S., et al. (2018). Connective tissue growth factor induces renal fibrosis via epidermal growth factor receptor activation. *J. Pathol.* *244* :
- Riser, B.L., Najmabadi, F., Perbal, B., Peterson, D.R., Rambow, J.A., Riser, M.L., et al. (2009). CCN3 (NOV) is a negative regulator of CCN2 (CTGF) and a novel endogenous inhibitor of the fibrotic pathway in an in vitro model of renal disease. *Am. J. Pathol.*
- Rodriguez-Díez, R., Rodriguez-Díez, R.R., Rayego-Mateos, S., Suarez-Alvarez, B., Lavoz, C., Stark Aroeira, L., et al. (2013). The C-terminal module IV of connective tissue growth factor is a novel immune modulator of the Th17 response. *Lab. Investig.* *93* :
- Rodrigues-Diez, R.R., Garcia-Redondo, A.B., Orejudo, M., Rodrigues-Diez, R., Briones, A.M., Bosch-Panadero, E., et al. (2015). The C-terminal module IV of connective tissue growth factor, through EGFR/Nox1 signaling, activates the NF- κ B pathway and proinflammatory factors in vascular smooth muscle cells. *Antioxidants Redox Signal.*
- Rodriguez-Vita, J., Sanchez-Lopez, E., Esteban, V., Ruperez, M., Egado, J., and Ruiz-Ortega, M. (2005). Angiotensin II activates the Smad pathway in vascular smooth muscle cells by a transforming growth factor-beta-independent mechanism. *Circulation* *111* : 2509–2517.
- Ruiz-Ortega, M., Rodriguez-Vita, J., Sanchez-Lopez, E., Carvajal, G., and Egado, J. (2007a). TGF-beta signaling in vascular fibrosis. *Cardiovasc. Res.* *74* : 196–206.
- Ruiz-Ortega, M., Rodríguez-Vita, J., Sanchez-Lopez, E., Carvajal, G., and Egado, J. (2007b). TGF- β signaling in vascular fibrosis. *Cardiovasc. Res.*
- Rupérez, M., Lorenzo, Ó., Blanco-Colio, L.M., Esteban, V., Egado, J., and Ruiz-Ortega, M. (2003). Connective tissue growth factor is a mediator of angiotensin II-induced fibrosis. *Circulation*.
- Shakil Ahmed, M., Gravning, J., Martinov, V.N., Lueder, T.G. von, Edvardsen, T., Czibik, G., et al. (2011). Mechanisms of novel cardioprotective functions of CCN2/CTGF in myocardial ischemia-reperfusion injury. *Am. J. Physiol. - Hear. Circ. Physiol.*
- Szabó, Z., Magga, J., Alakoski, T., Ulvila, J., Piuhola, J., Vainio, L., et al. (2014). Connective tissue growth factor inhibition attenuates left ventricular remodeling and dysfunction in pressure overload-induced heart failure. *Hypertension*.
- Thirunavukkarasu, S., Khan, N.S., Song, C.Y., Ghafoor, H.U., Brand, D.D., Gonzalez, F.J., et al. (2016). Cytochrome P450 1B1 Contributes to the Development of Angiotensin II-Induced Aortic Aneurysm in Male Apoe^{-/-} Mice. *Am. J. Pathol.*
- Thompson, A., Cooper, J.A., Fabricius, M., Humphries, S.E., Ashton, H.A., and Hafez, H. (2010). An analysis of drug modulation of abdominal aortic aneurysm growth through 25 years of surveillance. *J. Vasc. Surg.*
- Trachet, B., Fraga-Silva, R.A., Piersigilli, A., Tedgui, A., Sordet-Dessimoz, J., Astolfo, A., et al. (2015). Dissecting abdominal aortic aneurysm in Ang II-infused mice: Suprarenal branch ruptures and apparent luminal dilatation. *Cardiovasc. Res.*
- Wang, R., Xu, Y.J., Liu, X.S., Zeng, D.X., and Xiang, M. (2011). Knockdown of connective tissue growth factor by plasmid-based short hairpin RNA prevented pulmonary vascular remodeling in cigarette smoke-exposed rats. *Arch. Biochem. Biophys.*
- Wang, Y., Ait-Oufella, H., Herbin, O., Bonnin, P., Ramkhalawon, B., Taleb, S., et al. (2010). TGF- β activity protects against inflammatory aortic aneurysm progression and complications in angiotensin II-infused mice.

J. Clin. Invest.

Williams, H., Wadey, K.S., Frankow, A., Blythe, H.C., Forbes, T., Johnson, J.L., et al. (2021). Aneurysm severity is suppressed by deletion of CCN4. *J. Cell Commun. Signal.*

Yanagisawa, H., and Wagenseil, J. (2020). Elastic fibers and biomechanics of the aorta: Insights from mouse studies. *Matrix Biol.*

Zhang, C., Voort, D. Van Der, Shi, H., Zhang, R., Qing, Y., Hiraoka, S., et al. (2016). Matricellular protein CCN3 mitigates abdominal aortic aneurysm. *J. Clin. Invest.*

Zoppi, N., Chiarelli, N., Ritelli, M., and Colombi, M. (2018). Multifaced roles of the $\alpha\text{v}\beta\text{3}$ integrin in ehlers–danlos and arterial tortuosity syndromes’ dermal fibroblasts. *Int. J. Mol. Sci.*

TABLES

Table 1: List of the 67 deregulated genes (Q-value < 0.5; n-fold > 0.6) from the WT vs. CTGF-KO comparative analysis used to perform the Gene Ontology (GO) enrichment analysis.

Hosted file

image1.emf available at <https://authorea.com/users/325853/articles/528934-ccn2-deletion-predisposes-to-aortic-aneurysm-formation-and-death-in-mice-which-is-partially-reduced-by-mineralocorticoid-receptor-antagonist-treatment>

Table 2: GO enrichment analysis using 67 deregulated genes (Q-value < 0.5; n-fold > 0.6) from WT vs. CTGF-KO comparative analysis. Only terms with p-value adjusted by benjamini procedure <0.05 are included.

Hosted file

image2.emf available at <https://authorea.com/users/325853/articles/528934-ccn2-deletion-predisposes-to-aortic-aneurysm-formation-and-death-in-mice-which-is-partially-reduced-by-mineralocorticoid-receptor-antagonist-treatment>

FIGURE LEGENDS

Figure 1. CCN2 deficiency decreases mice survival following angiotensin II (Ang II) administration as a result of aortic aneurysm development and rupture. Wild-type (WT) and CCN2-KO mice were infused with Ang II for 15 days. Survival, aneurysm generation and blood pressure were analyzed. **A**, Kaplan-Meier survival curve showed a dramatic increase in mortality in Ang II-infused CCN2-KO mice. **B**, representative images of clean whole aorta showing thoracoabdominal aneurysms (TAAAs) generation in CCN2-KO mice infused with Ang II at end of follow-up. **C**, Evaluation of aneurysm appearance. Larger TAAA formation was found in 92 % of Ang II-infused CCN2-KO mice and smaller abdominal aneurysm (AbA) was observed in 30% and 8% of CCN2-KO and WT + Ang II mice respectively. **D**, Time-course of blood pressure changes in all mice groups since the first tamoxifen injection (Day -21) showed that Ang II increased blood pressure independently of the presence or absence of CCN2, as well as CCN2 deficiency decreased normal systolic blood pressure. Data are showed as box-and-whisker plots, with 75th and 25th percentiles; bars represent maximal and minimal values. n=8-13 mice per group.

Figure 2. CCN2 deficiency induces early aneurysm formation in mice in response to Ang II administration. Daily magnetic resonance imaging (MRI) assessments allowed a time-course analysis showing early aneurysm formation in Ang II-infused CCN2-KO mice. MRI experiments were followed only until 96 hours to avoid excessive mortality. Studies were done in a 1 cm aortic section proximal to the superior mesenteric artery (SMA) origin. **A**, Representative axial MRI images showing an increase in the total aortic area and a reduction in the minimal aortic lumen 48 hours after Ang II administration in CCN2-KO mice. Time-course quantification of **B**total aortic area (please note the different scale for the 96h panel),

C lumen area, **D** maximum total area and **E** minimum lumen area of the 1cm SMA analyzed. n= 4 mice per group. Data are shown as mean \pm SEM. * p < 0.05 increased *vs* . WT; # p < 0.05 decreased *vs* . WT.

Figure 3. CCN2 deficiency predisposes to TAAA formation in response to Ang II administration in mice. Ultrasound scanning was performed in live WT and CCN2-KO mice infused or not with Ang II, and evaluated at the start and the end point (0 and 15 days) of Ang II administration. **A**, representative ultrasound images. **B**, measurements of maximal diameters of TAsA, TDsA and AbA from all mice groups. Red dashed lines indicate the lumen boundary, and the yellow dashed lines indicate the lumen diameter. n = 5 mice per group. Data are showed as box-and-whisker plots, with 75th and 25th percentiles; bars represent maximal and minimal values.

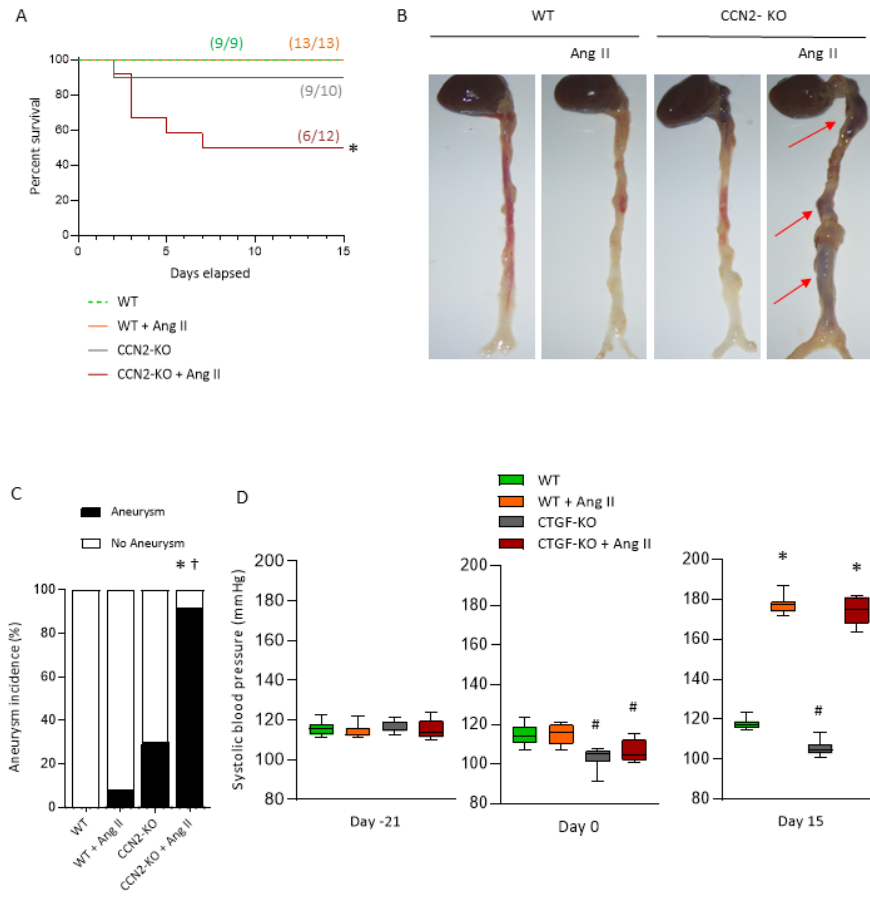
Figure 4. CCN2 deficiency promotes aortic structural and composition changes which are exacerbated in response to Ang II administration. **A**, Representative images of the aortic structure evaluated by Hematoxylin/Eosin (HE) at 10X and their magnification at 40X. *Considering aneurysms size, a lower magnification (4X) image was included in the CCN2-KO + Ang II group. Aneurysms were characterized by elastic lamina rupture and aortic wall dissection with extravasation of red blood cells outside the muscle layer forming a neo-lumen. An inflammatory cell infiltration in the border of the dissected aortic wall and reduced cellularity of the muscular layer were also observed in aneurysms. Figures show a representative picture of 6-8 mice per group. **B**, Representative images of aortic Van Gieson staining showing internal elastic lamina disrupted zones in CCN2-KO mice with or without Ang II infusion (Black arrows). **C**, Representative images of transmission electron microscopy (TEM) (2000X) confirming aortic elastic layers' disruption in absence of CCN2, boxed in red and magnified at 15000X below. EL= Elastic layer. Scale bars: 100 μ m at 10X objective and 20 μ m at 40X in histology; 10 μ m at 2000X and 1 μ m at 15000X in MET.

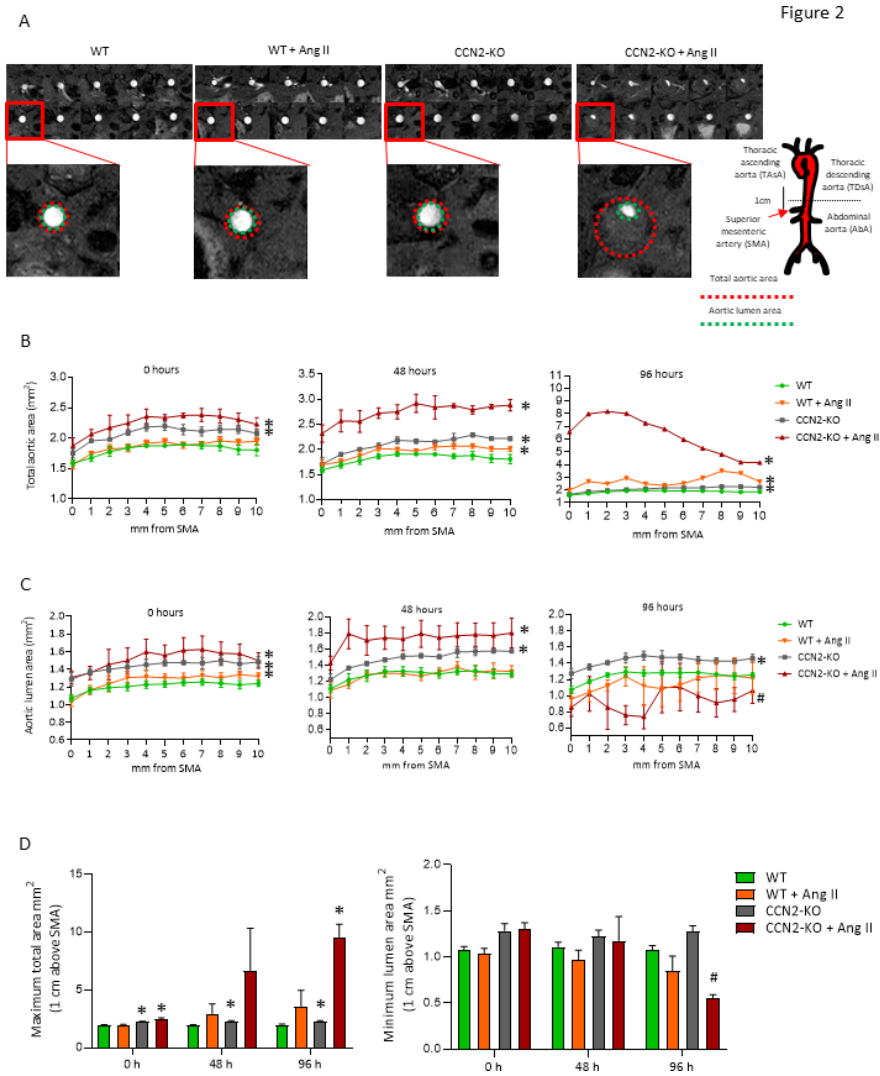
Figure 5. CCN2 deletion increases vascular matrix metalloproteinases (MMPs). MMPs activities or levels were evaluated in total aortic protein lysates. **A**, Representative MMP-2 and -9 gel zymography (upper panel) and quantification (lower panel) showing elevated MMP activities in the CCN2-KO group and increased activity following Ang II infusion. **B**. Representative image (upper panel) and quantification (lower panel) of MMP-8 western blot showing increased MMP-8 protein expression in total aortic protein extracts from the CCN2-KO group both treated or not with Ang II. **C**. *In situ* MMP activity was evaluated in paraffin-preserved aortas by the DQ-Gelatin fluorogenic substrate assay. Aortas of CCN2-KO and Ang II-infused WT mice displayed similar fluorescence intensity (green signal, observed between elastic layers), whereas there was a broadly distributed green signal in CCN2-KO + Ang II mice. n= 5-10 mice per group. Data are shown as mean \pm SEM. * p < 0.05 increased *vs* . WT; # p < 0.05 decreased *vs* . WT. + p < 0.05 *vs* . CCN2-KO. \$ p < 0.05 *vs* . CCN2-KO + Ang II.

Figure 6. Aorta transcriptomic study. **A**, Heat map diagram showing the two-way hierarchical clustering of genes for each group of mice. Each column represents the pooled mRNA obtained from 8-10 aortas per group. **B**, Heat map diagram showing the two-way hierarchical clustering of genes comparing just CCN2-KO mice *vs* WT.

Figure 7. Mineralocorticoid receptor blockade by spironolactone improves survival, aneurysm appearance rates and ameliorates aortic vascular function changes observed in Ang II-infused CCN2-KO mice. Spironolactone (SP) was started at the time of CCN2 deletion in the CCN2-KO + Ang II group. SP (50mg/kg/day) was intraperitoneally injected in alternate days until the end of follow-up. **A**, Kaplan-Meier survival curve showed less mortality in the CCN2-KO + Ang II group treated with SP compared to no SP treatment. **B**, SP decreased the percentage of aneurysm appearance in Ang II-infused CCN2-KO mice. **C**, SP did not prevent Ang II-induced blood pressure levels elevation. Data are showed as box-and-whisker plots, with 75th and 25th percentiles; bars represent maximal and minimal values. n=8-10 mice per group. **D**, Representative MMP-2 and 9 gel zymography (upper panel) and quantification (lower panel) showing a mild not significant MMP2 and MMP9 activity reduction in the CCN2-KO + Ang II group treated with SP. n= 7-10 mice per group.

Figure 1





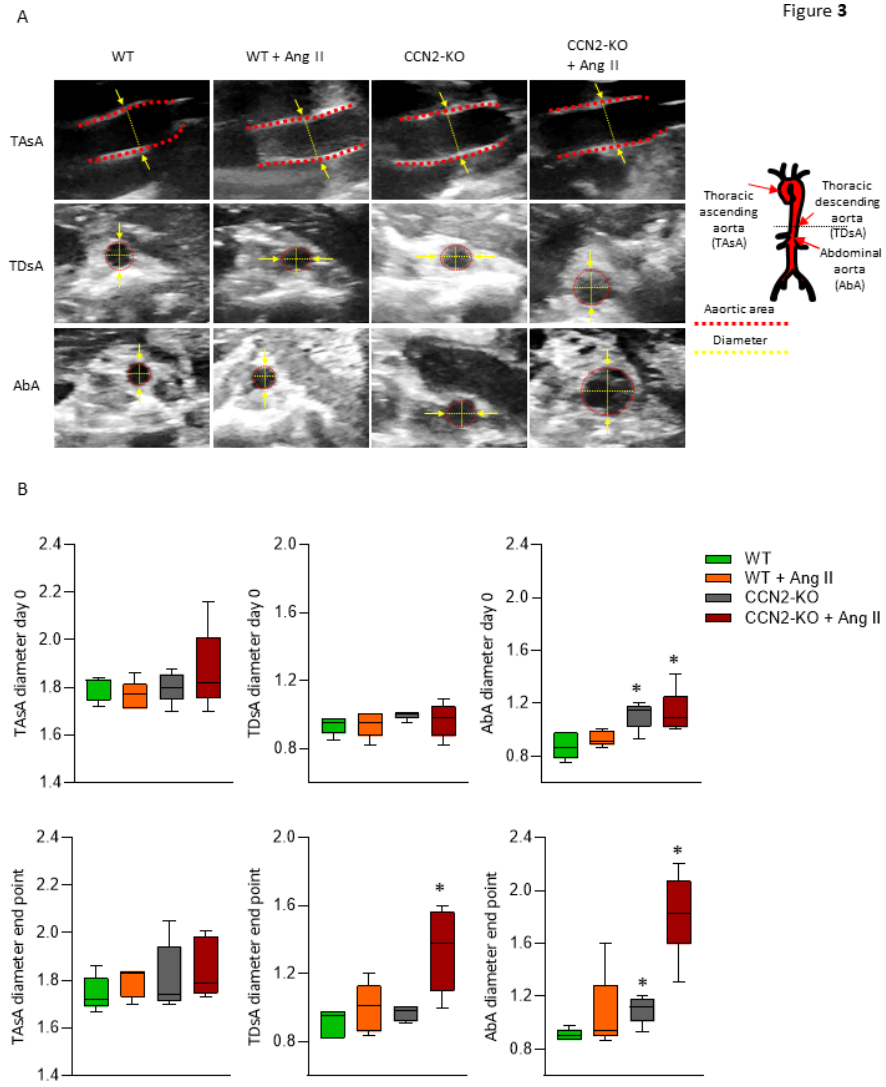


Figure 4

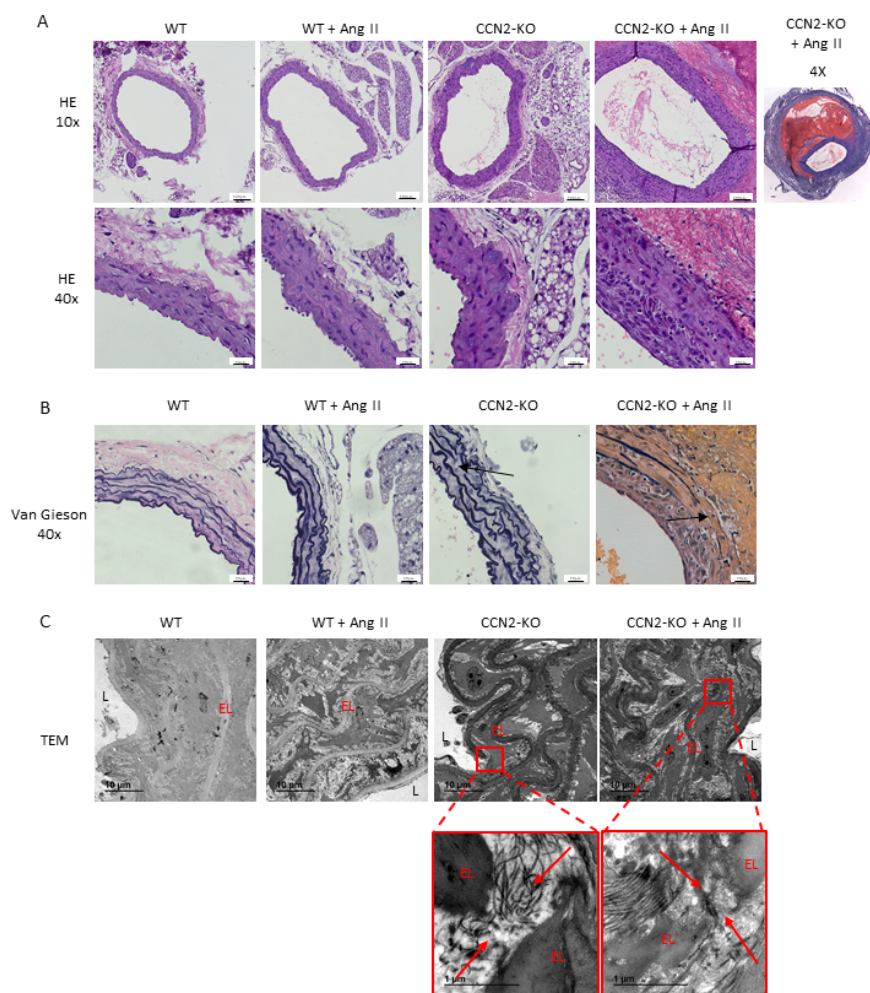


Figure 5

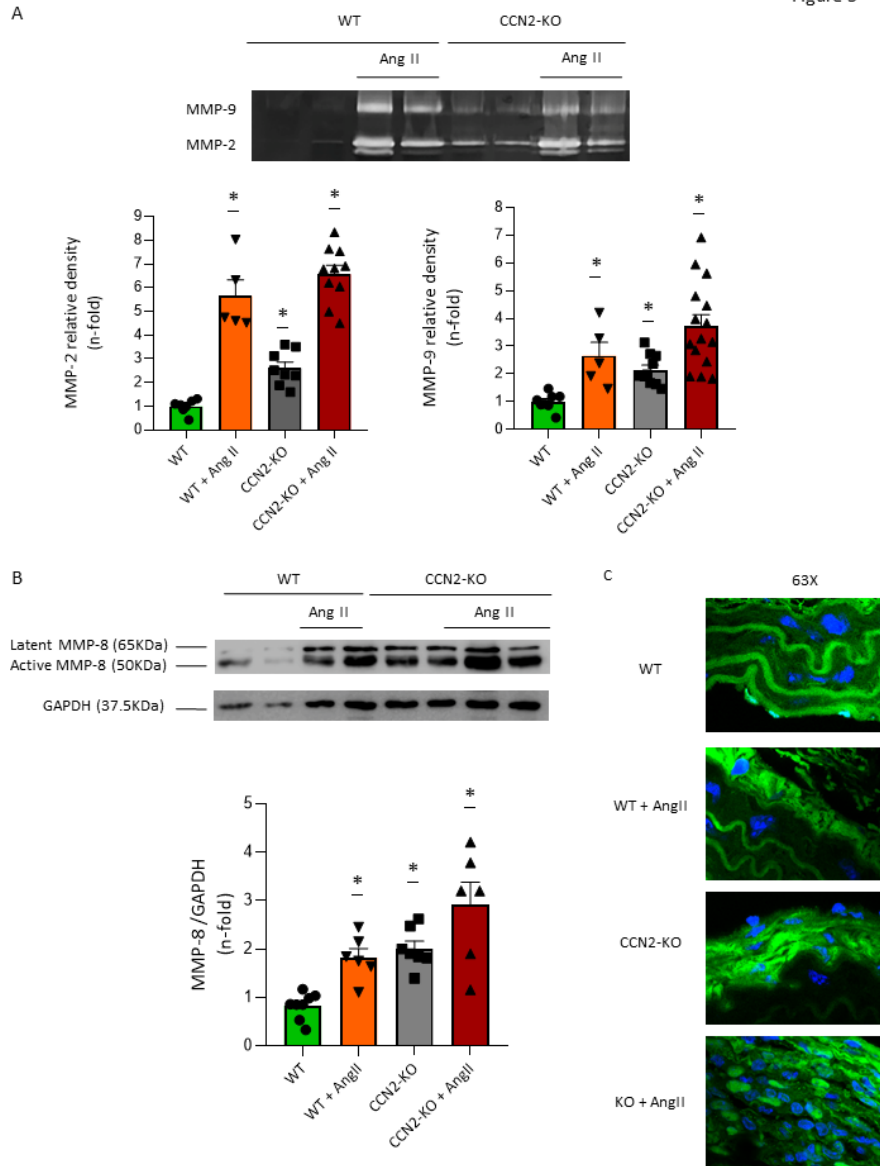


Figure 6

